# Electron precipitation coincident with ELF/VLF wave bursts

M. Walt

Starlab, Department of Electrical Engineering, Stanford University, Stanford, California, USA

H. D. Voss

Department of Physics, Taylor University, Upland, Indiana, USA

J. Pickett

Department of Physics, University of Iowa, Iowa City, Iowa, USA

[1]   On 15 October 1999, charged particle and plasma wave detectors on the Polar satellite observed an enhancement in precipitating energetic electrons coincident with an ELF/VLF electromagnetic emission. Assuming that the electromagnetic wave was field aligned and scattered trapped electrons by first-order cyclotron resonance near the equatorial plane, the resulting pitch angle distribution of precipitating electrons was calculated. For reasonable values of the cold plasma density and the wave intensity at the equatorial plane, the calculated precipitation agrees with measurements for an equatorial interaction region approximately 1000 km in length.   *INDEX TERMS:* 7867 Space Plasma Physics: Wave/particle interactions; 2471 Ionosphere: Plasma waves and instabilities; 2716 Magnetospheric Physics: Energetic particles, precipitating; 2736 Magnetospheric Physics: Magnetosphere/ionosphere interactions; *KEYWORDS:* wave-particle interactions, precipitation, plasma waves

## 1.   Introduction

[2]   Electron precipitation accompanying wave activity has been observed as chorus bursts coincident with auroral luminosity [*Helliwell et al.*, 1980] and X-ray production [*Rosenberg et al.*, 1971]. Also, whistler waves from lightning flashes have been detected on the ground in coincidence with electron precipitation observed from a satellite [*Voss et al.*, 1984, 1998] and with transient ionization in the upper atmosphere in thousands of cases [see, e.g., *Burgess and Inan*, 1993]. However, in situ observations of the wave bursts and associated particle precipitation are rare [*Skoug et al.*, 1996]. Satellite measurements of these events offer the possibility of comparing the electron spectra and angular deflections with wave characteristics and thus further clarifying transient particle precipitation events in the magnetosphere. Wave-particle events are believed to be the dominant loss mechanism for trapped electrons, but quantitative comparisons of theory and experiment during individual precipitation events are needed to be confident the mechanism is understood. In particular the size of the equatorial interaction region is uncertain, and it is not known whether the quasilinear treatment of particle diffusion is adequate.

[3]   This type of wave-particle coordinated measurement was planned for the Polar satellite using the Plasma Wave Instrument (PWI) [*Gurnett et al.*, 1995] to measure waves and the Source/Loss Cone Particle Spectrometer (SEPS) [*Blake et al.*, 1995] to make detailed pitch angle distribution measurements of energetic electrons near and inside the

bounce loss cone. Unfortunately, before SEPS could be adequately configured a component in PWI's power supply failed, resulting in an ''open'' circuit which prevented current from flowing to the digital logic. However, when the spacecraft environment becomes very cold for extended periods of time in the fall during eclipse of the spacecraft by the Earth, the open circuit closes partially. This contact supplies enough power to the low-rate processor to operate on an intermittent basis. This condition occurred during the fall of 1999, and a total of approximately 30 hours of wave data were obtained in short, scattered intervals. These data were examined for wave bursts and coincident changes in the trapped electron distributions. One isolated ELF/VLF burst accompanied by transient electron precipitation was recorded on 15 October 1999, when POLAR was at $L = 4.1$, at a magnetic latitude of $-50°$, and at a magnetic local time of 11:39, based on an offset, tilted dipole field model. This paper reports on the characteristics of the waves and particle distributions associated with this event.

## 2.   Observations
### 2.1.   Plasma Wave Data

[4]   Figure 1 shows a spectrogram of the electric and magnetic wave fields obtained by the PWI Multichannel Analyzer (MCA) at the time of the ELF/VLF pulse. The MCA consists of two receivers, each one sampling either the electric or magnetic wave field at all frequencies simultaneously. The two receivers are duty cycled, such that one cycle consists of sampling only the electric field waveform for 736 ms, followed by sampling only the magnetic field waveform for 515 ms, followed by a 74-ms rest period when neither waveform is sampled, for a total
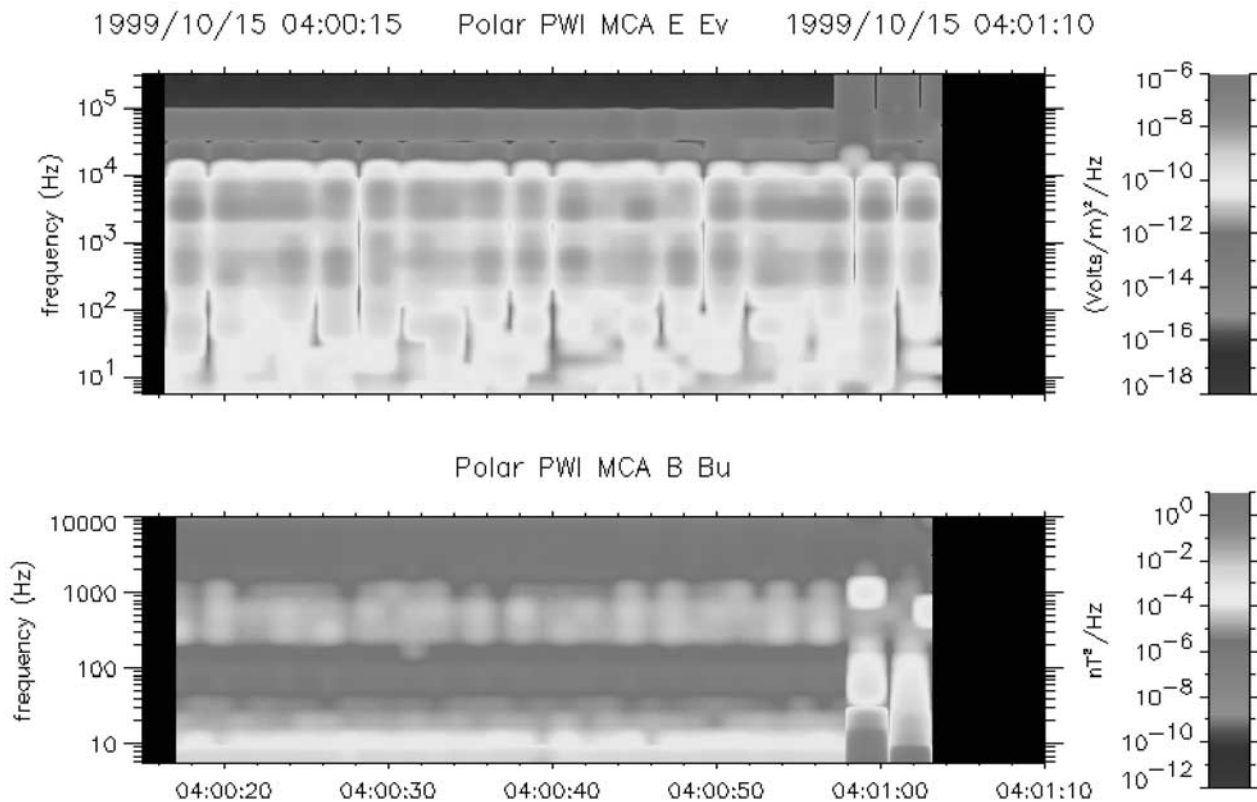
**Figure 1.** Spectrogram of 46 s of ELF/VLF data obtained by PWI on 15 October 1999. The pulse of interest occurred near 0400:58 UT. Data acquisition ended at 0401:03. See color version of this figure at back of this issue.

cycle time of about 1.3 s. Because the electric and magnetic wave fields are not sampled simultaneously, electromagnetic wave bursts that occur on timescales less than 500 ms will probably be observed in only the one receiver that is sampling at the time of the burst. At about 0400:59 UT the magnetic field spectral density over the range 5 Hz, the lowest frequency measured, to 100 Hz increased by at least an order of magnitude as shown in Figure 1 (bottom). In addition to the broadband bursts, two narrowband bursts were detected in the magnetic spectra, one at 0400:59 UT at a frequency around 1000 Hz, and one at 0401:03 at a frequency near 700 Hz, with power spectral densities that nearly reached $10^{-3}$ nT$^2$ Hz$^{-1}$. These narrowband bursts are distinct from the broadband bursts just discussed and distinct from the modulated emission which covers the frequency range of about 200 Hz to 2 kHz and which is observed through the entire time period shown in Figure 1 (bottom).

[5] The electric field data in Figure 1 (top) are less well defined but also show an enhancement starting at about 0400:57. At this time, wave electric field emissions are observed over the entire frequency range, 5 Hz to 311 kHz. In addition, the low-frequency waves (<100 Hz) appear to be slightly more intense. It is likely that more than one type of emission is detected, but it is impossible to resolve them since the waveforms are not available. Clearly, the two narrowband bursts observed in the magnetic spectra at 0400:59 and 0401:03 UT at 1000 and 700 Hz are not

apparent in the electric field spectra. Either their electric field components are at or below the intensity level of other emissions detected at these frequencies or the narrowband bursts occur on timescales less than 500 ms, which is most likely [see *Pickett et al.*, 2001]. Prior to and during the enhancement, electric field emissions are observed covering the range 200 Hz to 20 kHz. Some of this emission appears to be modulated at the half-spin period (3 s) which is typical of hiss-type emissions.

[6] The broadband wave transient observed in the magnetic spectrum at the lower frequencies appears to be the same type of emission observed by *Gurnett et al.* [1984] using Dynamics-Explorer 1 data. They described this emission as an intense broadband spectrum of low-frequency waves (frequency <100 Hz) accompanying 100 eV to 10 keV auroral electron precipitation and field-aligned currents. For the event in Figure 1, the broadband magnetic noise is observed at frequencies up to about the proton cyclotron frequency ($\sim$162 Hz at this position). Because the waveforms associated with this burst are not available, it is not known whether this burst as observed in the frequency domain is the result of an emission that is spread over a broad frequency range, or whether it is a result of a single pulse-type of waveform that will manifest itself as a broad band in the frequency domain, with the highest intensity at the lowest frequency. The broadband emission observed in the wave electric field (200 Hz to 20 kHz) and in the wave magnetic field (200 Hz to 2 kHz) prior to and after the
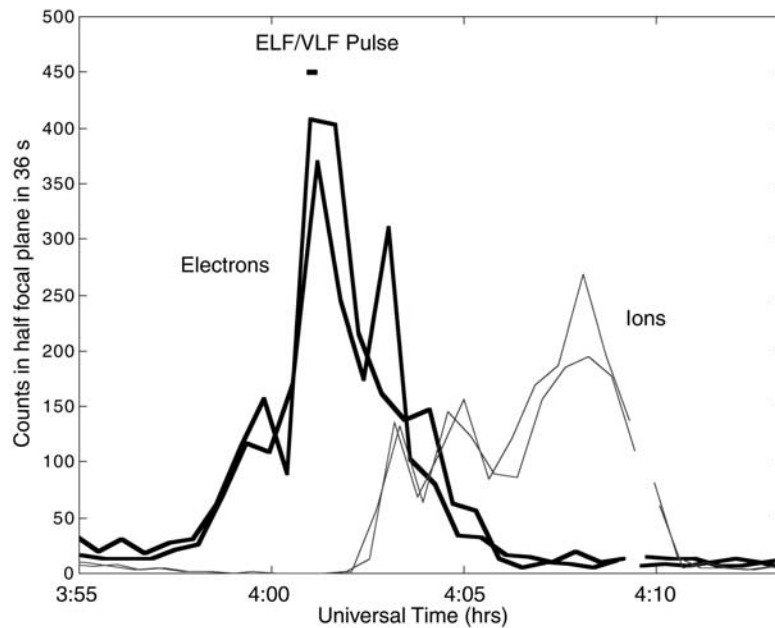
**Figure 2.** Electron and ion count rates observed in the bounce loss cone near the time of the ELF/VLF pulse. Thick lines denote counts from the two half planes of the electron detector, since each half plane accumulates counts over slightly different time periods. Thin lines give similar data for the ion detector. Note that ion fluxes in the loss cone are very low during the time of the ELF/VLF pulse.

enhancement may be hiss or ELF noise bands and is similar to that reported by *Gurnett et al.* [1984] in conjunction with the broadband spectrum of low-frequency waves

[7] The discrete, narrowband, magnetic bursts at about 1000 and 700 Hz are in the frequency range between the proton and electron cyclotron frequencies and are of primary interest here as they can resonate at the equator with 150-keV electrons. The PWI power supply ceased to operate after about 0401:03 UT, so it is not known whether the bursts continued after that time. Several other impulses of this character were seen during October 1999, but this case is the only one in which SEPS was oriented to look at particles in the loss cone.

## 2.2. Particle Precipitation Data

[8] The SEPS particle detectors used here were a proton and electron telescope, each consisting of a pinhole aperture followed by a focal plane matrix of 128 Si sensors. The overall fields of view of the detectors were about $20° \times 20°$, and each pixel sensor had an angular resolution of about $1.5°$. The proton telescope had a sweeping magnet at the aperture to exclude electrons. Each focal plane was divided electronically into two rectangular segments which cover the same pitch angle range if the SEPS axis is aligned with the magnetic field. Each segment was read out every 36 s, which is therefore the basic time resolution of the instrument. However, since the read times of the two segments of each telescope were separated by 9 s, some additional time information is available. The energy range of the electron telescope extended from about 155 keV to about 300 and the proton telescope was sensitive between 155 and 450 keV. Each proton and electron pulse was pulse height analyzed with electronic channel widths of about 39 keV. However, because of detector noise the effective width of each channel

was about 90 keV. During the time interval of interest here both telescopes were pointing upward nearly parallel to the geomagnetic field and therefore observed downward going particles.

[9] The electron and proton responses during a time interval including the wave event are plotted in Figure 2, where the time duration of the ELF/VLF pulse is indicated by the short horizontal bar at the top of the chart. These particles are in or near the bounce loss cone as SEPS was aligned nearly parallel to the magnetic field line and the local loss cone angle was about $26°$. Each point on the intensity versus time plot denotes the total counts recorded in a half focal plane during the 36 s before the time indicated on the plot. Lines are shown separately for each half plane of the electron and ion telescopes. Note that the ion fluxes in the loss cone are zero during the electron precipitation event, so the electron data are not contaminated by ions entering the electron detector. The ion enhancements after 0402 UT are of unknown origin as wave data are not available for that time. The electron data are replotted on an expanded timescale in Figure 3 where each horizontal bar indicates the total counts accumulated by each detector half plane during the 36-s recording period. The observed time duration of the ELF/VLF pulse is indicated by the horizontal bar near the bottom of Figure 3, although the emission may well have persisted after PWI ceased to function. Note that the three highest count rate intervals overlap the ELF/VLF pulse.

[10] The electron angular distribution at maximum intensity is plotted in Figure 4 where the crosses denote the electron fluxes at 155 keV as a function of equatorial pitch angle. Each symbol indicates the measurement by one detector pixel. Since counts are accumulated for 37 s, the flux values, which correspond to the times of the two
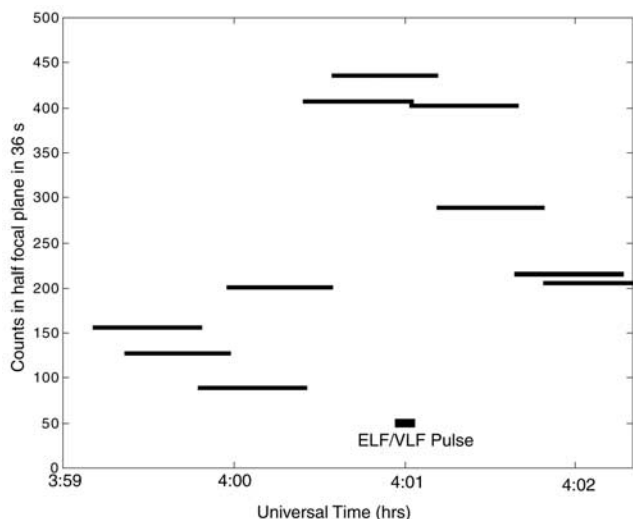
**Figure 3.** Time-expanded view of Figure 2 showing precise time correspondence between the electron enhancement and the ELF/VLF emission.

highest bars in Figure 3, are averages over 37 s. The local magnetic field direction was measured by the Magnetic Field Experiment on the Polar satellite, and the measured electron distribution was transformed to the equatorial plane using an offset, tilted dipole field model. Since the equato-

rial loss cone in the Northern (Southern) Hemisphere for an atmospheric cutoff at 100 km is 5.39° (5.61°), nearly all the observed pitch angles are within the local bounce loss cone.

[11] Measurements at other energy channels gave similar angular distributions and indicate that the energy spectrum of precipitating electrons falls rapidly with increasing energy. SEPS data can be fit by an exponential with e-folding energy of about 30 keV. Because of the detector noise, these data are also consistent with a monoenergetic peak near 150 keV. Although the spectrum of trapped electrons at this location could not be measured by SEPS, at $L = 4$ and at 150 keV the trapped fluxes have e-folding energies of about 200 keV [*Vette*, 1991]. Thus the precipitated spectrum is much less energetic than the trapped electron component, indicating that the scattering process favors the lower energy electrons.

## 3. Analysis

[12] The precise time association of the electrons and the VLF waves strongly suggests that the precipitating electrons were scattered into the loss cone by the wave event. Pitch angle distributions of trapped and precipitating electrons in equilibrium with plasmaspheric hiss were calculated by *Davidson and Walt* [1977] for a number of broadband wave amplitudes. The highest amplitude used in these calculations was a broadband wave field of 0.18 nT. If this wave field extended over 1 kHz in frequency, it would correspond
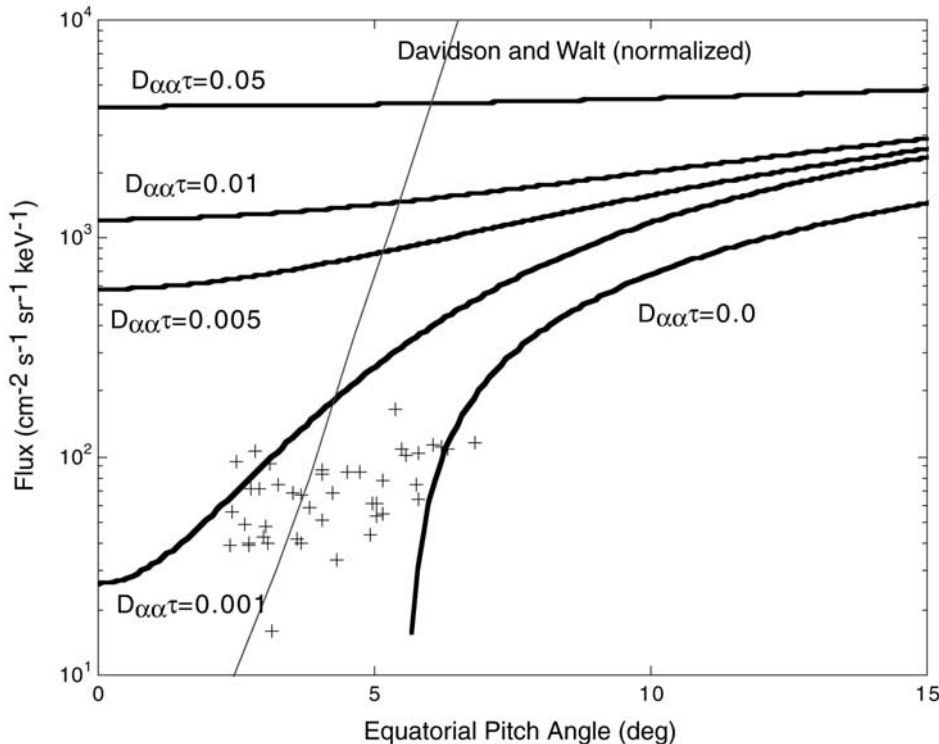


**Figure 4.** Measured electron pitch angle distribution (crosses) and theoretical values based on assumed values of $D_{\alpha\alpha}\tau$. The pitch angle scattering is assumed to take place near the equator and is caused by cyclotron interaction of trapped electrons with the wave pulse. The thin curve [*Davidson and Walt*, 1977] is based on quiet time pitch angle diffusion in plasmaspheric hiss and is normalized for easier comparison of flux gradients.

to an average power spectral density of $3 \times 10^{-5}$ (nT)$^2$ Hz$^{-1}$. The thin line in Figure 4 denotes the normalized electron distribution computed for this wave field. It is apparent that the observed pitch angle distribution is much flatter, indicating that the observed scattering is much stronger than calculated and that the electrons are scattered deep into the loss cone during a single half bounce. The observed wave intensity near 1 kHz is about $5 \times 10^{-4}$ (nT)$^2$ Hz$^{-1}$ (see Figure 1), which is much stronger than the highest value used by Davidson and Walt. It is therefore not surprising that the observed scattering is stronger.

[13] To estimate the scattering in this case we assume the wave originated near the equator, propagated toward both poles and scattered the trapped electrons. The wave-particle interaction region is assumed to be near the equator. We also assume that a simplified diffusion equation applies with a constant diffusion coefficient. For whistler waves propagating parallel to the magnetic field the local diffusion equation and diffusion coefficient, $D_{\alpha\alpha}$, are given by *Kennel and Petschek* [1966], *Gendrin* [1968], and others.

$$\frac{\partial f}{\partial t} = \frac{1}{\sin\alpha}\frac{\partial}{\partial\alpha}\left[D_{\alpha\alpha}\sin\alpha\frac{\partial f}{\partial\alpha}\right] \qquad (1)$$

$$D_{\alpha\alpha} = \frac{1}{2}\left(\frac{e}{m}\right)^2\left(\frac{v_g}{v_z}\right)P_b(\Omega - kv_z), \qquad (2)$$

where $f$ is the electron distribution function, $\alpha$ is the local pitch angle, $e$ and $m$ are the charge and mass of the electron, $v_g$ is the wave group velocity, $v_z$ is the electron velocity parallel to the ambient magnetic field, and $P_b(\Omega - kv_z)$ is the power spectral density of the wave magnetic field evaluated at the resonant frequency. For this simple case where electrons at small pitch angles interact only near the equator during one pass, the bounce averaged diffusion equation is not needed. Although we do not know the equatorial cold plasma density or the wave normal angle, 150-keV electrons with small pitch angles at $L = 4.1$ will resonate with waves between 100 Hz and 1 kHz for a range of cold plasma densities and wave normal angles. Cold plasma measurements are not available, but it is likely that Polar is outside the plasmasphere. The largest $Kp$ value during the preceding 24 hours is 5, which would place the plasmapause at $L = 3.3$ using the empirical formula of *Carpenter and Anderson* [1992]. In this calculation the cold electron density at the equator is assumed to be 40 cm$^{-3}$, which would allow 800-Hz waves at wave normal angles of $0°$ to resonate with 150-keV electrons.

[14] We solve equation (1) as an initial value problem by separation of variables. For small $\alpha$ the angular eigenfunctions are Bessel functions of the first kind and of zero order. The initial distribution function was approximated by

$$f(\alpha, t = 0) = 1.3 \times 10^4$$
$$\cdot \sin\left[\left(\frac{\pi}{2}\right)(\alpha - \alpha_{LC})/(90° - \alpha_{LC})\right] \qquad \alpha_{LC} < \alpha < 90°$$
$$f(\alpha, t = 0) = 0 \qquad \alpha < \alpha_{LC}, \qquad (3)$$

where $\alpha_{LC}$ is the loss cone angle of $5.6°$. The multiplicative constant is taken from *Vette* [1991] and is the differential, directional flux at 150 keV and $90°$ on the equator at $L = 4$.

The diffusion takes place near the equator during the time $\tau$ required for a particle to pass through the interaction region. The distributions for $t > 0$ are therefore parameterized by the product $D_{\alpha\alpha}\tau$.

[15] In Figure 4, angular distributions are shown for values of $D_{\alpha\alpha}\tau$ ranging from zero to $D_{\alpha\alpha}\tau = 0.05$, a $D_{\alpha\alpha}\tau = 0$ corresponding to the reservoir of trapped electrons before encountering the wave. The experimental values are expected to fall below the theory since the measured fluxes are averaged over 37 s while the duration of the ELF/VLF pulse and electron precipitation was much less. To compare absolute values, one should multiply the measured fluxes by the ratio of 37 s to the unknown pulse duration. However, the slopes of the fluxes on the logarithmic scale should be directly comparable. Comparing theoretical and experimental values of the slopes of $f(\alpha)$ inside the loss cone indicates that values of $D_{\alpha\alpha}\tau$ near 0.005 or 0.01 give agreement with the observations.

[16] These values of $D_{\alpha\alpha}\tau$ are quite plausible. With $P_b(\Omega - kv_z)$ of $5 \times 10^{-4}$ (nT)$^2$ Hz$^{-1}$ at 700 Hz and the appropriate values of $v_g$, and $v_z$, one obtains $D_{\alpha\alpha} \approx 1$ s$^{-1}$ from equation (2). The interaction time $\tau$ required is therefore between 0.005 and 0.01 s, corresponding to an interaction length of about $1000-2000$ km. *Helliwell and Inan* [1982] estimated the interaction region at $L = 4$ outside the plasmasphere to be about 1485 km based on the distance in which the wave and particles remained nearly in phase. Considering the many uncertainties in this calculation such as the equatorial plasma density and the intensity and time dependence of the wave field at the equator, this result is quite reasonable.

## 4. Conclusion

[17] A short burst of precipitating 155-keV electrons which accompanied an enhancement of ELF/VLF waves was observed from the POLAR satellite on 15 October 1999. The angular distribution of the precipitating electrons was consistent with trapped electrons being scattered by the electromagnetic wave as they passed through an equatorial interaction region. In this case, the quasilinear diffusion theory with a diffusion coefficient based on electrons interacting with a whistler mode wave with zero wave normal angle gives satisfactory agreement with experiment.
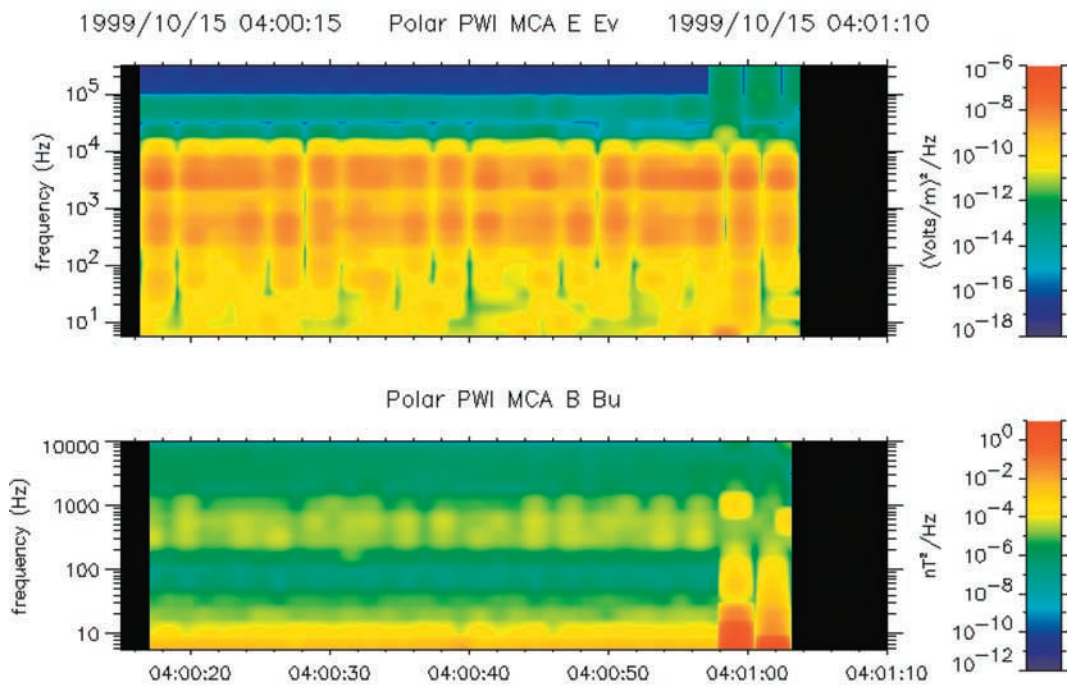
## References

Blake, J. B., et al., Comprehensive energetic particle and pitch angle distribution experiment on POLAR, in *The Global Geospace Mission*, edited by C. T. Russell, Kluwer Acad., Norwell, Mass., 1995.
Burgess, W. C., and U. S. Inan, The role of ducted whistlers in the precipitation loss and equilibrium flux of radiation belt electrons, *J. Geophys. Res.*, *98*, 15,643, 1993.
Carpenter, D. L., and R. R. Anderson, An ISEE/Whistler model of equatorial electron density in the magnetosphere, *J. Geophys. Res.*, *97*, 1097, 1992.

Davidson, G., and M. Walt, Loss cone distributions of radiation belt electrons, *J. Geophys. Res.*, *82*, 48, 1977.

Gendrin, R., Pitch angle diffusion of low energy protons due to gyroresonant interactions with hydromagnetic waves, *J. Atmos. Terr. Res.*, *30*, 1313, 1968.

Gurnett, D. A., R. L. Huff, J. D. Menietti, J. L. Burch, J. D. Winningham, and S. D. Shawhan, Correlated low-frequency electric and magnetic noise along the auroral field lines, *J. Geophys. Res.*, *89*, 8971, 1984.

Gurnett, D., et al., POLAR plasma wave instrument, *Space Sci. Rev.*, *71*, 597, 1995.

Helliwell, R. A., and U. S. Inan, ELF wave growth and discrete emission triggering in the magnetosphere: A feedback model, *J. Geophys. Res.*, *87*, 3537, 1982.

Helliwell, R. A., S. B. Mende, J. H. Doolittle, W. C. Armstrong, and D. L. Carpenter, Correlations between λ4278 optical emissions and VLF wave events observed at L~4 in the Antarctic, *J. Geophys. Res.*, *85*, 3376, 1980.

Kennel, C. F., and H. E. Petschek, Limit on stably trapped particle fluxes, *J. Geophys. Res.*, *71*, 1, 1966.

Pickett, J. S., J. R. Franz, J. D. Scudder, J. D. Menietti, D. A. Gurnett, G. B. Hospodarsky, R. M. Braunger, P. M. Kintner, and W. S. Kurth, Plasma waves observed in the cusp turbulent boundary layer: An analysis of high time resolution wave and particle measurements from the Polar spacecraft, *J. Geophys. Res.*, *106*, 19,081, 2001.

Rosenberg, T. J., R. A. Helliwell, and J. P. Katsufrakis, Electron precipitation associated with discrete very low frequency emissions, *J. Geophys. Res.*, *76*, 8445, 1971.

Skoug, R. M., S. Datta, M. P. McCarthy, and G. K. Parks, A cyclotron resonance model of VLF chorus emissions detected during electron microburst precipitation, *J. Geophys. Res.*, *101*, 21,481, 1996.

Vette, J. I., The AE-8 Trapped Electron Model Environment, *NSSDC/WDC-A-R&S 91-24*, NASA Goddard Space Flight Cent., Greenbelt, Md., 1991.

Voss, H. D., et al., Lightning-induced electron precipitation, *Nature*, *312*, 740, 1984.

Voss, H. D., M. Walt, W. L. Imhof, J. Mobilia, and U. S. Inan, Satellite observations of lightning-induced electron precipitation, *J. Geophys. Res.*, *103*, 11,725, 1998.

———————
J. Pickett, Department of Physics, University of Iowa, Iowa City, IA 52242, USA.

H. D. Voss, Department of Physics, Taylor University, Upland, IN 46989, USA.

M. Walt, Starlab, Department of Electrical Engineering, Stanford University, Packard Building, Stanford, CA 94305, USA. (walt@nova.stanford.edu)

**Figure 1.** Spectrogram of 46 s of ELF/VLF data obtained by PWI on 15 October 1999. The pulse of interest occurred near 0400:58 UT. Data acquisition ended at 0401:03.